Selective loss of function variants in *IL6ST* cause Hyper-IgE syndrome with distinct impairments of T-cell phenotype and function

Tala Shahin,[1,2*] Dominik Aschenbrenner,[3*] Deniz Cagdas,[4,5*] Sevgi Köstel Bal,[1,2,6] Cecilia Domínguez Conde,[1,2] Wojciech Garncarz,[1,2] David Medgyesi,[1,2] Tobias Schwerd,[3,7] Betül Karaatmaca,[4] Pınar Gur Cetinkaya,[4] Saliha Esenboga,[4] Stephen R. F. Twigg,[8] Andrew Cant,[9] Andrew O. M. Wilkie,[8] Ilhan Tezcan,[4,5] Holm H. Uhlig[3,10] and Kaan Boztug[1,2,11,12]

[1]Ludwig Boltzmann Institute for Rare and Undiagnosed Diseases, Vienna, Austria; [2]CeMM Research Center for Molecular Medicine of the Austrian Academy of Sciences, Vienna, Austria; [3]Translational Gastroenterology Unit, John Radcliffe Hospital, University of Oxford, UK; [4]Section of Pediatric Immunology, Ihsan Doğramacı Children's Hospital, Hacettepe University, Ankara, Turkey; [5]Institute of Child Health, Hacettepe University, Ankara, Turkey; [6]Department of Pediatric Allergy and Immunology, Ankara University School of Medicine, Cebeci, Turkey; [7]Dr. von Hauner Children's Hospital, Ludwig-Maximilians-University of Munich, Germany; [8]Clinical Genetics Group, MRC Weatherall Institute of Molecular Medicine, John Radcliffe Hospital, University of Oxford, UK; [9]Institute of Cellular Medicine, Newcastle University, Newcastle upon Tyne, UK; [10]Department of Paediatrics, University of Oxford, UK; [11]Department of Pediatrics and Adolescent Medicine, Medical University of Vienna, Austria and [12]St. Anna Kinderspital and Children's Cancer Research Institute, Department of Pediatrics, Medical University of Vienna, Austria

**TSh, DA and DC contributed equally to this work. #HHU and KB are co-senior authors.*

 doi:10.3324/haematol.2018.194233

Received: March 26, 2018.

Accepted: October 3, 2018.

Pre-published: October 11, 2018.

Correspondence:

KAAN BOTZUG - kaan.boztug@rud.lbg.ac.at

HOLM H. UHLIG - holm.uhlig@ndm.ox.ac.uk

Supplementary Data

Methods

Exome sequencing and data analysis

Whole exome sequencing was performed using the TrueSeq Rapid Exome kit, Illumina HiSeq3000 system and the cBot cluster generator. Burrows-Wheeler Aligner was used to align reads against version 19 of the human genome as a reference. VCF.Filter tool[1] was used to filter out variants (annotated by SNPEFF) with a minor allele frequency (MAF) >0.01 in 1000 Genomes, ExAC or dbSNP. An internal database was also used to filter out recurrent variants. In the resulting list of variants homozygous changes were then subjected to prioritization using the combined annotation dependent depletion (CADD) tool[2] to predict deleteriousness.

Sanger sequencing

Validation and segregation of the GP130 variant P498L was performed on DNA from P^{P498L} and family members by Sanger sequencing. DNA from the deceased sister and twin brothers was not available. The following primers were designed for amplification and sequencing: Forward: 5'-CCGAACAGTAGGTCCTTTGG-3', Reverse: 5'-CCACTGCATTGGCAATACTT-3'.

Patient-derived cells and KO cell line

T Lymphoblasts: T Lymphoblasts were generated by feeder cell-mediated T cell expansion. Irradiated feeder cells (PBMCs and JY cells) were added in a 1:1 ratio to patient PMBCs in T cell media (RPMI 1640 (Gibco) + 5% human serum + 1% penicillin/streptomycin + 1% Hepes) supplemented with IL-2 (100U, ImmunoTools) and PHA (1µg/ml; Sigma). T cells were allowed to expand for two weeks.

Epstein-Barr virus transformed lymphoblastoid cells (EBV-LCL): PBMCs freshly isolated from the patient, mother and healthy donor blood were incubated with EBV virus supernatant for one day followed by addition of 1 µg/ml cyclosporin A. Cells were grown in RPMI 1640 medium (Gibco) supplemented with 10% heat-inactivated fetal bovine serum (HI-FBS), 1% L-glutamine and 1% penicillin/streptomycin (all from Invitrogen).

CRISPR/Cas9 GP130 KO HEK293 cell line: The GP130 KO HEK293 cell line was established in house as described previously[3]. Cells were grown in DMEM with glutamine (Sigma) supplemented with 10% FCS (Sigma), 1% sodium-pyruvate (Gibco), 1% non-essential amino acids (Gibco), 1% penicillin/streptomycin (Gibco).

Plasmid and lentivirus production for reconstitution experiments

pcDNA3.1(+) vector coding for wildtype (WT) or mutant GP130, and wildtype IL-6RA and IL-11RA were purchased from GenScript and expanded in Stbl3 *E. coli* (Thermo Fisher) according to standard protocols. Plasmids were purified using the EndoFree Plasmid Maxi Kit (Qiagen) or E.Z.N.A.® Endo-Free Plasmid Maxi Kit (Omega bio-tek).

For ectopic expression of WT *IL6ST* in patient-derived fibroblasts, infectious lentiviral particles were generated as described previously[3] with some adaptations. pLENTI7.3V5-DEST (Geneart; Thermo

Fisher) carrying WT *IL6ST* was co-transfected into HEK293 cells using Lipofectamine2000 (Invitrogen) and the ViraPower lentiviral packaging mix (Invitrogen) according to the manufactures' instructions. HEK293 cell supernatants were filtered by passing through a 0.45μm filter and added to primary fibroblasts in 6-well plate cultures. Transduction efficiency was ~70% based on EmGFP expression. After 24 hours incubation cells were serum starved for 2 hours, followed by cytokine stimulation and p-STAT staining, as described in the Methods section of the article.

Transcription factor profiling

The expression of T cell lineage-specifying transcription factors was analyzed following surface and intracellular co-staining of 0.5-1x10^6 total PBMCs. Cells were stained for surface markers and for the exclusion of dead cells as described below, fixed and permeabilized using the transcription factor staining buffer set (eBioscience), followed by flow cytometry analysis. The expression of transcription factors was detected with the following antibodies: FOXP3, GATA3, RORγt and TBET.

TSNE-clustering

t-Distributed Stochastic Neighbor Embedding (TSNE)-based analysis was performed on FCS files compensated for spillover between channels and gated on live $CD3^+CD4^+CD8^-$ or live $CD3^+CD8^+CD4^-$ single cells and randomly down-sampled to 10.000 ($CD4^+$) or 3000 ($CD8^+$) cells per sample. Individual FCS files were then concatenated to generate a single FCS file and subjected to tSNE unsupervised analysis using the FlowJo (Treestar) tSNE plugin[4,5] . The settings were: Iterations = 1000; Perplexity = 200; Eta = 20; Theta = 0.5. Clustering was performed on the following parameters: CD45RA, CD25, CD127, CCR4, CCR6, CCR7, CCR9, CCR10, CXCR3, CXCR5 and CRTh2. All patient T cell analysis were compared to matched 12-year old healthy donors samples (p.P498L) or 7-year old healthy donor samples (p.N404Y) that were stained and acquired on the same day.

Statistical analysis

In cases when three or more independent experiments were performed, an unpaired two-tailed student *t*-test or Mann-Whitney-test were performed on Prism (version 5 or 7; GraphPad software, Inc.).

Protein sequence alignment

Clustal Omega[6] was used to align multiple sequences from different species: NP002175 (Human), NP_001252920 (Macaque), NP_034690 (Mouse), NP_990202 (Chicken) and NP_001106976.

Supplementary Tables

Table S1. List of Antibodies used for p-STAT assays, GP130 expression, extracellular surface staining, intracellular cytokine staining (ICCS), transcription factor (TF) and chemokine receptor (CCR) profiling.

Antibody-Fluorophore	Clone	Producer	Purpose
CD3-FITC	UCHT1	Beckman Coulter	p-STAT Assay
CD4-BV605	RPA-T4	BD Pharmigen	
CD8-V450	RPA-T8	BD Horizon	
CD19-PECy7	J3-119	Beckman Coulter	
pSTAT1-BV421	4a (pY701)	BD Phosflow	
pSTAT2-FITC	Polyclonal (pY689)	Thermofisher	
pSTAT3-AF647	4/P-STAT3 (pY701)	BD Phosflow	
pSTAT4-PE	T693 (pY693)	BD Biosciences	
pSTAT5-PECy7	47/Stat5 (pY694)	BD Biosciences	
pSTAT6-PerCPCy5.5	18/P-Stat6 (pY641)	BD Biosciences	
IL-4-APC	MP4-25D2	BD Biosciences	ICCS
IL-10-PECy7	JES3-9D7	eBioscience	
IL-13-FITC	85BRD	eBioscience	
IL-17A-eF450	eBio64DEC17	eBioscience	
IL-22-PE	22URTI	eBioscience	
IFNγ-PE-Dazzle or FITC	4S.B3	Biolegend or eBiosciences	
TNFα-BV605	MAb11	Biolegend	
FOXP3-APC	PCH101	eBioscience	TF profiling
GATA3-AF488	TWAJ	eBioscience	
RORγT-PE or AF647	Q21-559	BD Biosciences	
TBET-BV711 or PerCPCy5.5	4B10	Biolegend	
CD130-BV421	AM64	BD Biosciences	GP130 expression
CD4-BV421	RPA-T4	BD Biosciences	
CD3-BV711, PECy5 or PE-Tr	UCHT1	BD Biosciences	Extracellular surface staining for ICCS, TF and CCR Profiling
CD3-APC-H7	*SK7*	BD Biosciences	

αβTCR-PerCPCy5.5	*IP26*	Biolegend	
CD4-BV510	*RPA-T4*	Biolegend	Extracellular surface staining for ICCS, TF and CCR Profiling
CD4-PECy7	SFCI12T4D11	Beckman Coulter	
CD8-AF700	*RPA-T8*	Biolegend	
CD8-V500	*RPA-T8*	BD Biosciences	
CD25-BV785	MA-A251	Biolegend	
CD25-PE	MA-A251	BD Biosciences	
CD45RA-BV650	HI100	Biolegend	
CD45RA-AF700	HI100	BD Biosciences	
CD127-BV570	A019D5	Biolegend	
CCR4-PECy7	1G1	BD Biosciences	
CCR6-BV605	G034E3	Biolegend	
CCR7-BV421	G043H7	Biolegend	
CCR7-PE-CF594	150503	BD Biosciences	
CCR9-APC	L053E8	Biolegend	
CCR10-PE	314305	R&D	
CXCR3-PECy5 or BV711	1C6	BD Biosciences	
CXCR5-PE-Dazzle	J252D4	Biolegend	
CRTh2-FITC	BM16	BD Biosciences	
GP130-BV421	*AM64*	BD Biosciences	

Table S2. NIH-HIES score calculated on the basis of the clinical manifestations of P^{P498L}.

Clinical Findings	***P^{P498L}***
Highest serum-IgE level (IU/ml)	10
Skin abscesses	0
Pneumonia (episodes over lifetime)	8
Parenchymal lung anomalies	8
Retained primary teeth	0
Scoliosis, maximum curvature	8
Fractures with minor trauma	0
Highest eosinophil count (cells/ml)	6
Characteristic face	2
Midline anomaly	0
Newborn rash	0
Eczema (worst stage)	4
Upper respiratory infections per year	2
Candidiasis	0
Other serious infections	4
Fatal infection	0
Hyperextensibility	2
Lymphoma	0
Increased nasal width	1
High palate	2
Young-age correction	0
Total score	57

Table S3. Summary of clinical manifestations present in P^{P498L} and P^{N404Y}.

Organ Affected	***Phenotype***	***P^{P498L}*** ***(12.5 years)***	***P^{N404Y}*** ***(7 years)***
Growth	Short stature (height < 3rd percentile)	✓	Not assessed
Skin	Eczema	✓	✓
Head and neck	Scaphocephaly (Craniosynostosis)	✓	✓
	Retained teeth	✓	✓
Bones and joints	Scoliosis (30° thoracolumbar curve)	✓	✓
	Flexion contracture of the small joints of the hands and elbows	✓	✓
	Hip dislocation	✓	✓
	Destructive arthropathy	✓	Not assessed
Infections	Recurrent upper respiratory tract infections	✓	✓
	Recurrent otitis media	✓	×
	Recurrent pneumonia, empyema and pneumatocele	✓	✓
	Bilateral keratitis	✓	✓
	Fungal lesions	✓	×
Nervous system	Mental motor retardation	✓	✓

Table S4. Homozygous, non-synonymous rare variants (minor allele frequency (MAF) <0.01 using the ExAC database) found in subject P^{P498L}. CADD algorithm was used to predict functional damage of variants.

Gene	*Chr*	*Position*	*Reference allele*	*Alternative allele*	*Amino acid change*	*dbSNP*	*MAF (ExAC)*	*CADD score*
IL6ST	5	55248137	G	A	P498L	.	NA	31.0
WDR36	5	110454719	A	G	D658G	rs34595252	4.209e-03	29.4
*APC**	5	112175240	G	C	E1317Q	rs1801166	4.126e-03	7.7
MCC	5	112720862	A	G	V73A	.	NA	25.6
HSD17B4	5	118850709	G	A	A516T	rs28943591	3.114e-03	23.0
GRM6	5	178418549	T	C	I245V	rs62638207	4.143e-03	19.7
CRB2	9	126133161	G	T	R610L	rs144365725	2.636e-04	11.2
SOHLH1	9	138590970	C	G	G23A	rs201456816	1.766e-04	7.2
C10orf99	10	85944516	G	T	Q80H	rs76221724	3.937e-03	24.2
CXCR5	11	118764497	A	C	T82P	rs202087123	8.236e-05	19.0
USP2	11	119243713	G	A	R160W	rs200291387	3.954e-04	22.8
LTB4R	14	24785092	G	T	A79S	rs34645221	4.876e-03	11.8
RBBP6	16	24581416	G	C	E1135D	rs112763526	4.945e-05	17.97
SLC5A11	16	24902246	G	A	A241T	.	NA	23.0
KIAA0556	16	27751497	G	A	E627K	rs186875199	1.450e-03	12.8
CLPTM1	19	45494509	A	G	Y478C	rs140564801	1.137e-03	28.7
PIGA	X	15349359	T	A	S232C	.	NA	25

* The nonsynonymous variant in APC (p.E1317Q) has been described in some patients with familial forms of polyposis coli and colorectal cancer in heterozygous forms[7,8]. The penetrance is not complete and homozygous forms have not been evaluated.

References

1. Müller H, Jimenez-Heredia R, Krolo A, et al. VCF.Filter: interactive prioritization of disease-linked genetic variants from sequencing data. Nucleic Acids Res 2017;45(W1):W567–W572.
2. Kircher M, Witten DM, Jain P, O'Roak BJ, Cooper GM, Shendure J. A general framework for estimating the relative pathogenicity of human genetic variants. Nat Genet 2014;46(3):310–315.
3. Schwerd T, Twigg SRF, Aschenbrenner D, et al. A biallelic mutation in IL6ST encoding the GP130 co-receptor causes immunodeficiency and craniosynostosis. J Exp Med 2017;214(9):2547–2562.
4. Maaten L van der, Hinton G. Visualizing Data using t-SNE. J Mach Learn Res

2008;9(Nov):2579–2605.

5. Wallach I, Lilien R. The protein–small-molecule database, a non-redundant structural resource for the analysis of protein-ligand binding. Bioinforma Orig Pap 2009;25(5):615–62010.

6. Sievers F, Wilm A, Dineen D, et al. Fast, scalable generation of high-quality protein multiple sequence alignments using Clustal Omega. Mol Syst Biol 2014;7(1):539–539.

7. Gismondi V, Bonelli L, Sciallero S, et al. Prevalence of the E1317Q Variant of the *APC* Gene in Italian Patients with Colorectal Adenomas. Genet Test 2002;6(4):313–317.

8. Lamlum H, Al Tassan N, Jaeger E, et al. Germline APC variants in patients with multiple colorectal adenomas, with evidence for the particular importance of E1317Q. Hum Mol Genet 2000;9(15):2215–2221.

Supplementary Figure Legends

Figure S1.

Functional assessment of STAT family members' phosphorylation in GP130^{P498L} T lymphoblasts. Bar graph summary of STAT1, STAT2, STAT3, STAT4, STAT5 and STAT6 phosphorylation following stimulation with 100 ng/ml (A) IL-6, (B) IL-27, (C) IL-4, (D) IL-12, (E) IL-21 or (F) IFNβ-in T lymphoblasts from P^{P498L} and two HDs. Data shown are from 2-3 independent experiments with 2 replicates each. t-test; *p<0.05, **p<0.01, ***p<0.001.

Figure S2.

Functional assessment of GP130^{P498L} fibroblast p-STAT1 response. (A) Dose-escalation curves showing relative mean fluorescence intensity (rMFI) of p-STAT1 after stimulation of P^{P498L} and HD fibroblasts as well as P^{P498L} fibroblasts transduced with wild-type (WT) GP130 with IL-6, IL-11, IL-27, LIF or OSM. Bar graphs (right) showing rMFI of fibroblasts upon stimulation with the highest concentration of the corresponding cytokine (3 (HD), 4 (p.P498L) and 2 (p.P498L + WT GP130) replicates of 2 independent experiments). (B) Dot-plot presentation of p-STAT1 and p-STAT3 co-stained fibroblasts according to (A) following stimulation with 100 ng/ml IL-6, IL-11, IL-27, LIF or OSM.

Figure S3.

Profiling of CD4$^+$ and CD8$^+$ T cells chemokine receptor expression. Bar graph summary of (A and B) CD4$^+$ and (C and D) CD8$^+$ memory T cells chemokine receptor surface expression shown as frequency of live CD3$^+$CD4$^+$CD25$^-$ or CD3$^+$CD8$^+$CD25$^-$ T cells, respectively. Mean + SEM; HD age-matched controls (9-14 years): n = 10-11, HD age-matched controls (6-7 years): n = 6-9, P^{P498L}: n = 2-5 independent replicates from PBMCs isolated at 3 distinct time points and at 7 and 4-month distance, P^{N404Y}: n = 3 replicates from 2 independent experiments and PBMCs taken at 5-month distance. Mann-Whitney test; *p<0.05, **p<0.01, ***p<0.001, ****p<0.0001. Some healthy donor control data shown was previously published[5].

Figure S4.

Phenotypic characterization of $CD8^+CCR6^+$ memory T cells. (A) Summary of frequencies of $TBET^+$ and $ROR\gamma t^+$ cells as assessed by intracellular staining and expressed as frequencies of $CD8^+$ memory T cells. Mean + SEM; HD (adult): n = 28, HD age-matched controls (9-14 years): n = 8, HD age-matched controls (6-7 years): n = 7, P^{P498L}: n = 4 replicates from two independent experiments from PBMCs isolated at two distinct time points and at 7-month distance, P^{N404Y}: n = 3 replicates from two independent experiments and PBMCs taken at 5-month distance. (B) Dot-plot showing the expression of CCR6 and RORγt in $CD8^+$ memory T cells. (C) Dot-plot presentation illustrating the expression of TBET and RORγt in $CD8^+$ memory T cells. Gates were set using naïve $CD8^+$ T cells as internal negative control.

Figure S5.

Evaluation of regulatory T cell frequencies. (A) Bar graph summary of $CD25^+FOXP3^+$ T cell frequencies gated on live $CD3^+CD4^+$ cells: mean + SD: HD (adult): n = 9, HD age-matched controls (9-14 years): n = 7, HD age-matched controls (6-7 years): n = 6, P^{P498L}: n = 3 independent replicates from PBMCs isolated at two distinct time points and at 7-month distance, P^{N404Y}: n = 3 replicates from two independent experiments and PBMCs taken at 5-month distance. (B) Dot-plot presentation of $CD25^+FOXP3^+$-gated T cell populations according to A.

Figure S6.

Gating strategy for the analysis of chemokine receptor expression and transcription factor expression in $CD4^+$ T cells. Dot plot examples are shown from one adult healthy donor.

Figure S7.

Bar graph summary showing percentages of cells expressing TBET, GATA3 or RORγt within CCR-enriched Th-cell subsets and $CD3^+CD4^+CD25^-$ naïve T cells: mean + SD: HD: n = 23, P^{P498L}: n = 5 independent replicates from PBMCs isolated at two distinct time points and at 7 and 4-month distance, P^{N404Y}: n = 3 replicates from 2 independent experiments and PBMCs taken at 5-month distance. Mann-Whitney test; *p<0.05, **p<0.01, ***p<0.001, ****p<0.0001.

Figure S1

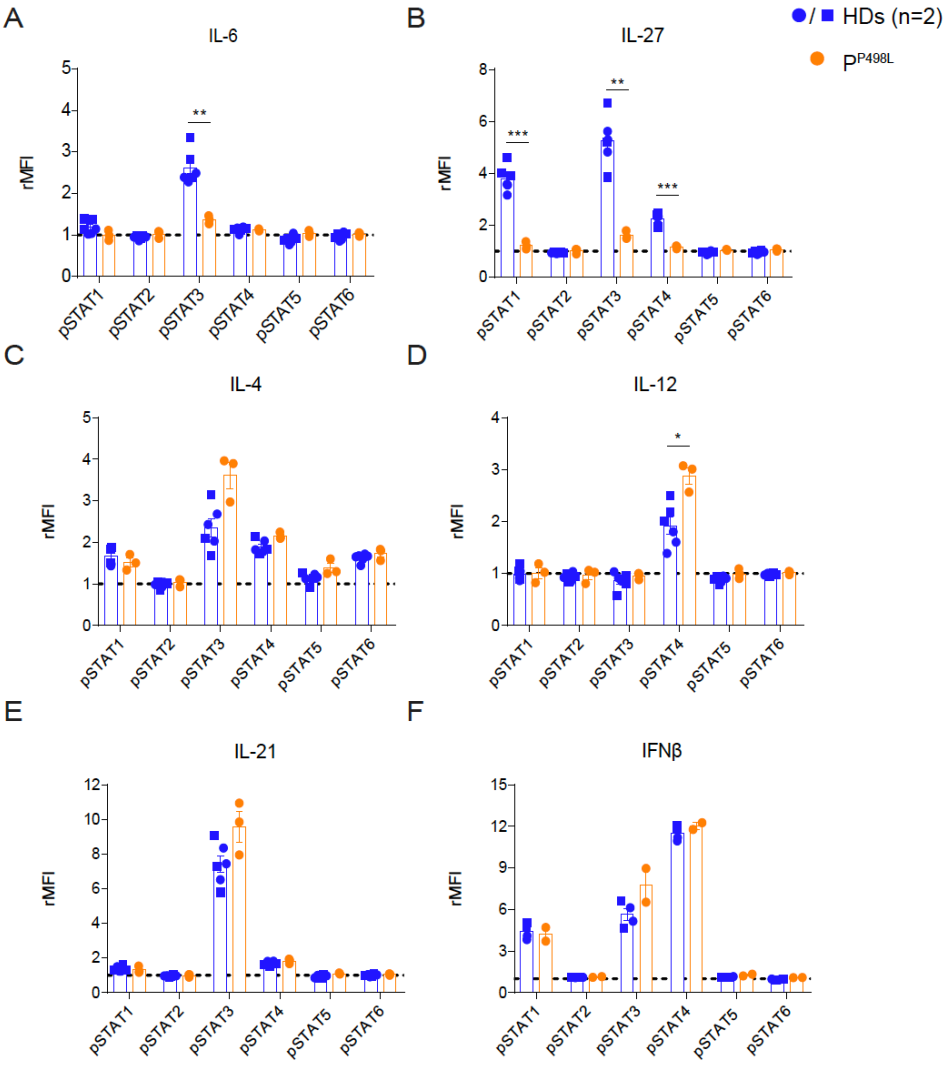
A
IL-6
rMFI
pSTAT1
pSTAT2
pSTAT3
pSTAT4
pSTAT5
pSTAT6
B
IL-27
C
IL-4
D
IL-12
E
IL-21
F
IFNβ
HDs (n=2)
P P498L

Figure S2

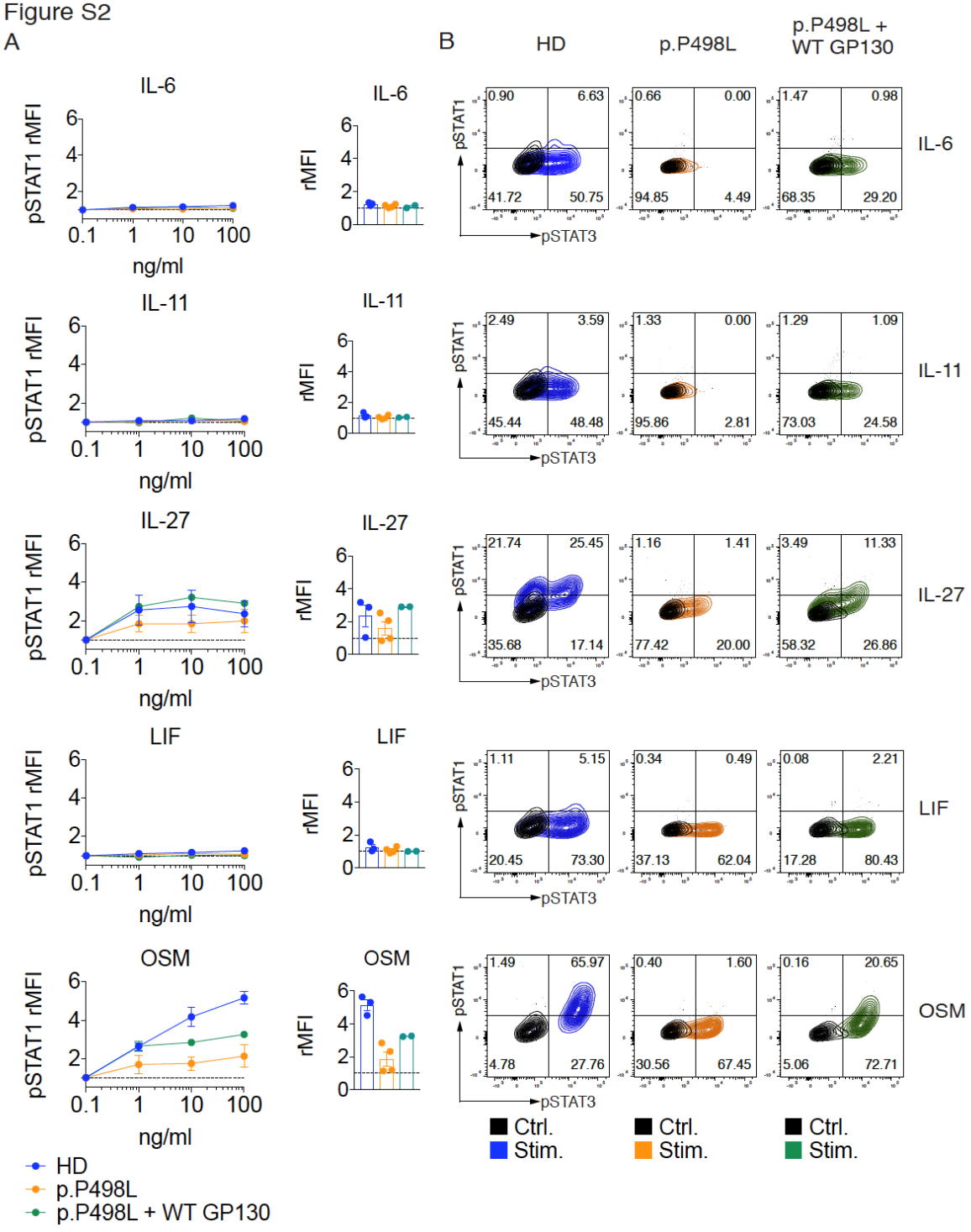
A
B
HD
p.P498L
p.P498L + WT GP130
IL-6
IL-11
IL-27
LIF
OSM
pSTAT1 rMFI
rMFI
ng/ml
0.1
1
10
100
pSTAT1
pSTAT3
0.90
6.63
41.72
50.75
0.66
0.00
94.85
4.49
1.47
0.98
68.35
29.20
2.49
3.59
45.44
48.48
1.33
0.00
95.86
2.81
1.29
1.09
73.03
24.58
21.74
25.45
35.68
17.14
1.16
1.41
77.42
20.00
3.49
11.33
58.32
26.86
1.11
5.15
20.45
73.30
0.34
0.49
37.13
62.04
0.08
2.21
17.28
80.43
1.49
65.97
4.78
27.76
0.40
1.60
30.56
67.45
0.16
20.65
5.06
72.71
Ctrl.
Stim.
Ctrl.
Stim.
Ctrl.
Stim.
HD
p.P498L
p.P498L + WT GP130

Figure S3

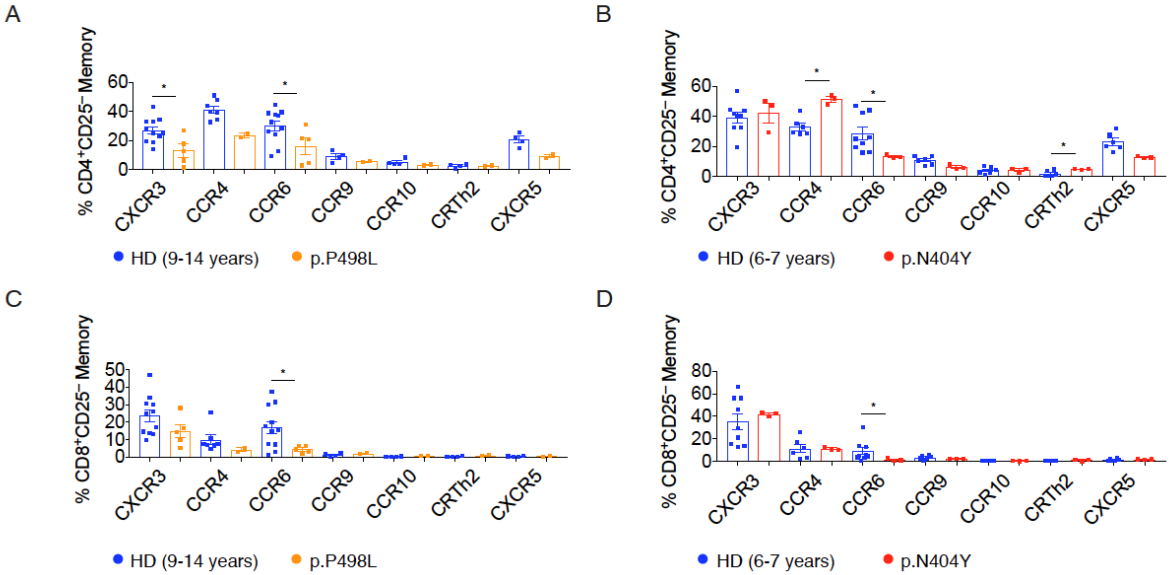
A
% CD4+CD25- Memory
60
40
20
0
*
*
CXCR3
CCR4
CCR6
CCR9
CCR10
CRTh2
CXCR5
HD (9-14 years)
p.P498L
B
% CD4+CD25- Memory
60
40
20
0
*
*
*
CXCR3
CCR4
CCR6
CCR9
CCR10
CRTh2
CXCR5
HD (6-7 years)
p.N404Y
C
% CD8+CD25- Memory
50
40
30
20
10
0
*
CXCR3
CCR4
CCR6
CCR9
CCR10
CRTh2
CXCR5
HD (9-14 years)
p.P498L
D
% CD8+CD25- Memory
80
60
40
20
0
*
CXCR3
CCR4
CCR6
CCR9
CCR10
CRTh2
CXCR5
HD (6-7 years)
p.N404Y

Figure S4

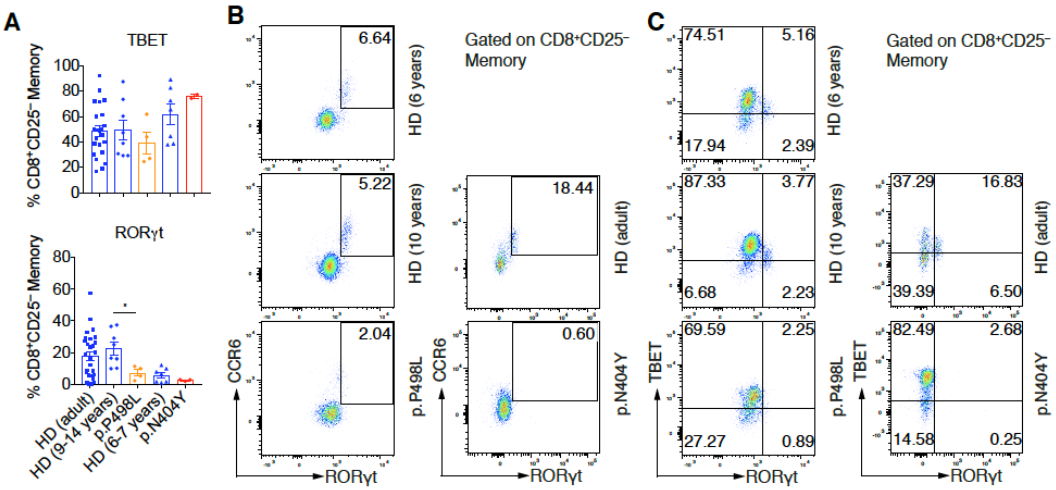
A
TBET
% CD8+CD25- Memory
RORγt
% CD8+CD25- Memory
HD (adult)
HD (9-14 years)
p.P498L
HD (6-7 years)
p.N404Y
B
Gated on CD8+CD25- Memory
6.64
5.22
2.04
18.44
0.60
HD (6 years)
HD (10 years)
HD (adult)
p.P498L
p.N404Y
CCR6
RORγt
C
74.51
5.16
17.94
2.39
87.33
3.77
6.68
2.23
69.59
2.25
27.27
0.89
37.29
16.83
39.39
6.50
82.49
2.68
14.58
0.25
TBET
RORγt

Figure S5

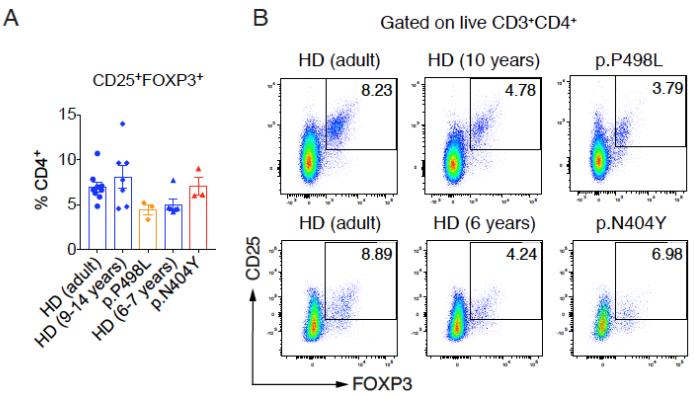
A
CD25+FOXP3+
% CD4+
15
10
5
0
HD (adult)
HD (9-14 years)
p.P498L
HD (6-7 years)
p.N404Y
B
Gated on live CD3+CD4+
HD (adult)
HD (10 years)
p.P498L
8.23
4.78
3.79
HD (adult)
HD (6 years)
p.N404Y
8.89
4.24
6.98
CD25
FOXP3

Figure S6

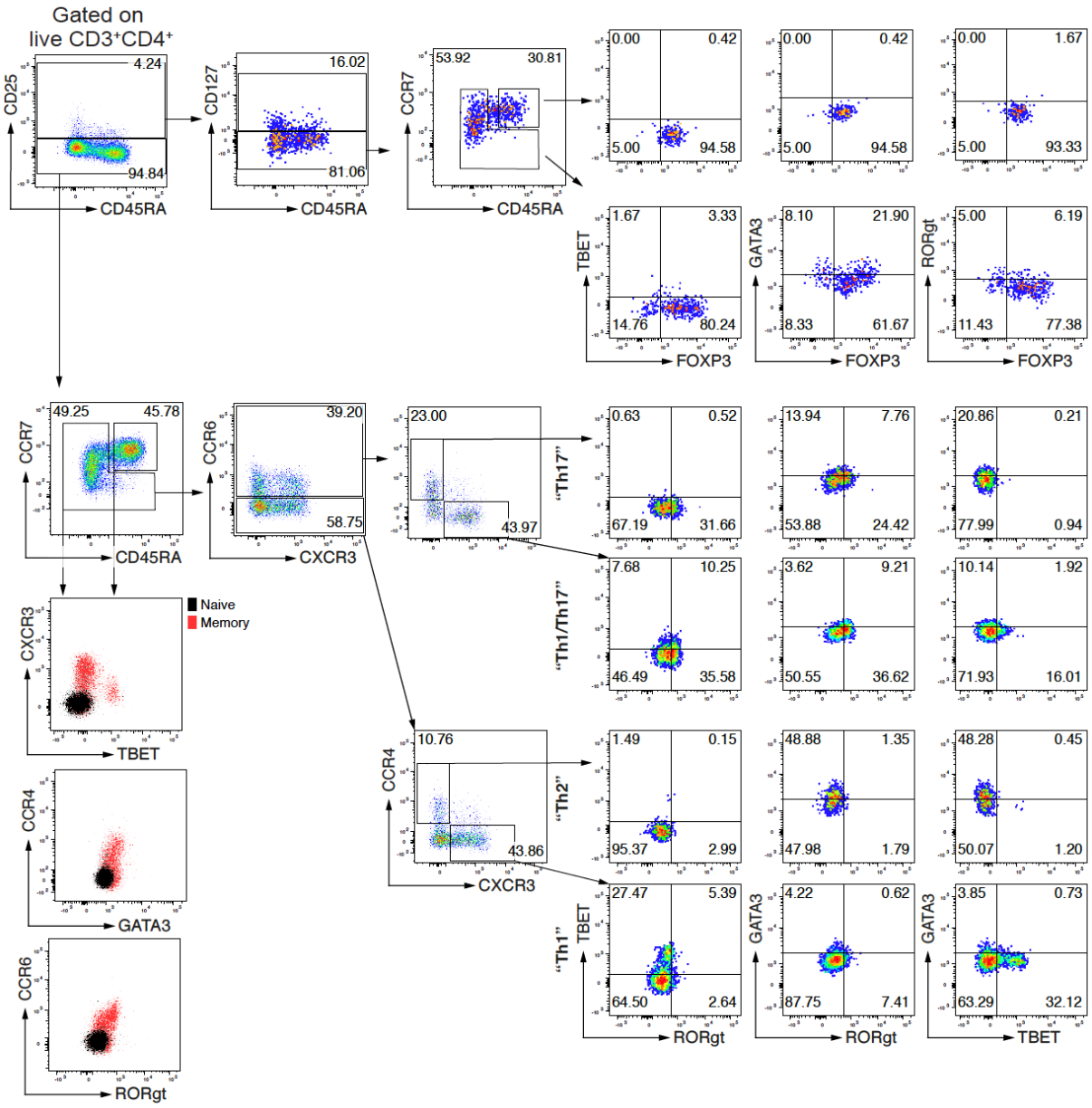
Gated on
live CD3+CD4+
CD25
4.24
94.84
CD45RA
CD127
16.02
81.06
CD45RA
CCR7
53.92
30.81
CD45RA
0.00
0.42
5.00
94.58
0.00
0.42
5.00
94.58
0.00
1.67
5.00
93.33
TBET
1.67
3.33
14.76
80.24
FOXP3
GATA3
8.10
21.90
8.33
61.67
FOXP3
RORgt
5.00
6.19
11.43
77.38
FOXP3
CCR7
49.25
45.78
CD45RA
CCR6
39.20
58.75
CXCR3
23.00
43.97
"Th17"
0.63
0.52
67.19
31.66
13.94
7.76
53.88
24.42
20.86
0.21
77.99
0.94
"Th1/Th17"
7.68
10.25
46.49
35.58
3.62
9.21
50.55
36.62
10.14
1.92
71.93
16.01
CXCR3
Naive
Memory
TBET
CCR4
10.76
43.86
CXCR3
"Th2"
1.49
0.15
95.37
2.99
48.88
1.35
47.98
1.79
48.28
0.45
50.07
1.20
"Th1"
TBET
27.47
5.39
64.50
2.64
RORgt
GATA3
4.22
0.62
87.75
7.41
RORgt
GATA3
3.85
0.73
63.29
32.12
TBET
CCR4
GATA3
CCR6
RORgt

Figure S7

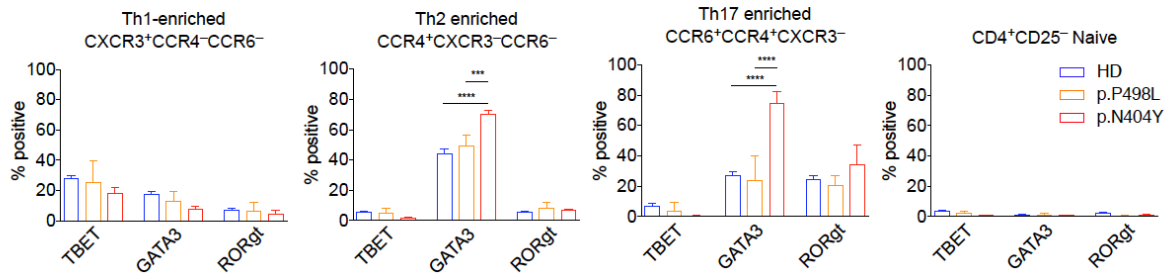
Th1-enriched
CXCR3+CCR4−CCR6−
Th2 enriched
CCR4+CXCR3−CCR6−
Th17 enriched
CCR6+CCR4+CXCR3−
CD4+CD25− Naive
% positive
100
80
60
40
20
0
TBET
GATA3
RORgt
***
****
****
****
HD
p.P498L
p.N404Y